

IMPLEMENTATION OF HIGH DIMENSION COLOUR TRANSFORM IN DOMAIN OF IMAGE PROCESSING

Anchal A. Khadse¹, Mr. M. H. Nerkar²

¹M.Tech student, Electronics and Telecommunication Engineering, Government College of Engineering, Jalgaon, Maharashtra, India

²Professor in Electronics and Telecommunication Engineering, Government College of Engineering, Jalgaon, Maharashtra, India

Abstract - Extraction of salient region from colour image is very useful nowadays so this topic deals with the study of salient region detection in an image with the help of high dimension colour transform algorithm. To extract salient region from the image it is necessary to design saliency map. For computation of saliency map, global and local features of the image are needed to find out. The creation of saliency map is a first approach of this work, and it is a linear combination of colours in high dimensional colour space. By mapping the low-dimensional red, green, and blue colour to a feature vector in a high-dimensional colour space, we show that we can composite an accurate saliency map by finding the optimal linear combination of colour coefficients in the high-dimensional colour space. The performance of our saliency estimation is improved by our second approach which is used to utilize relative location and colour contrast between superpixels as features and to resolve the saliency estimation from a trimap via a learning-based algorithm. We here used number of images as a trained dataset for analysis of different parameters in colour images.

Key Words: Salient Region; Superpixels; trimap; feature vector; HDCT method; Learning based algorithm.

1. INTRODUCTION

Synthesis of different components or elements form a meaningful region in an image is termed as salient region. A region is meant to be salient if it differs from its surrounding region. Saliency detection means detecting visually attracted regions in images. A main purpose behind a calculation of such region with the help of HDCT method is to know whether an object in an image attracts viewer's attention or not. A salient object can be identified due to many features present in it. They can be color, shape, gradient, edge and boundaries which are main characteristics for perception and processing of visual stimuli to human vision. In image processing we read about image pre-processing techniques which are important for several applications. Likewise salient region detection is one of a pre-processing method and useful for applications like image retrieval, object recognition, image retargeting, segmentation, photo collage, image quality assessment, image thumb nailing, and video compression.

As color is a very important visual cue to human, many salient region detection techniques are built upon distinctive color detection from an image. This project contains an approach to automatically detect salient regions in an image. First approach is to estimate the approximate locations of salient regions by using a tree-based classifier. A tree-based classifier classifies each superpixel as a foreground, background or unknown pixels. This classifier classifies those foreground and background regions into salient and non-salient regions with high confidence. The unknown region is classified with low confidence but that unknown region includes ambiguous features in it. All the three regions foreground, background as well as unknown regions forms an initial trimap, and our purpose is to resolve the ambiguousness from that unknown regions to calculate accurate saliency map. From the trimap, we can conclude to use two different methods, high-dimensional color transform (HDCT)-based method and local learning based method to estimate the saliency map. The results of these two methods will be combined together to form our final saliency map. Figure 1 shows examples of our saliency map and salient regions from trimap.

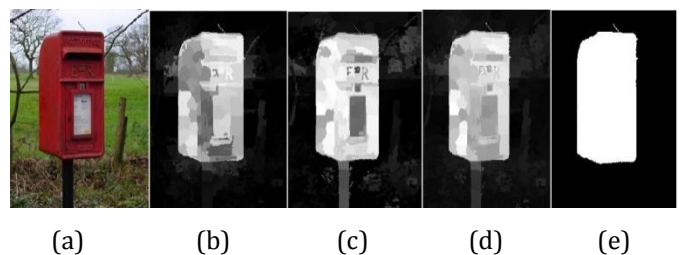


Fig -1: Example of our salient region detection method from a trimap. (a) Input. (b) Trimaps. (c) Saliency maps. (d) Salient region with final segmentation. (e) Ground truth.

2. LITERATURE REVIEW

The methodologies for deciding low-level saliency can be founded on natural models or computational models. Some methodologies consider saliency more than a few scales while other works on solitary scale. Here it is necessary to decide nearby balance of picture areas with its background support. As reported the HDCT-based

method presented is one of the top six algorithms in salient region detection. Local-contrast-based models detect salient regions by detecting rarity of image features in a small local region. In Itti et.al paper they [3] proposed a saliency detection method which utilizes visual filters called “center-surround difference” to compute local color contrast. Harel et al. [4] suggested a graph-based visual saliency (GBVS) model which is based on the Markovian approach on an activation map. This model examines the dissimilarity of center-surround feature histograms. Goferman et al. [5] combined global and local contrast saliency to improve detection performance. Klein and Frintrap [6] utilized information theory and defined the saliency of an image using the Kullback-Leibler divergence (KLD). The KLD measures the center-surround difference to combine different image features to compute the saliency. Hou et al. [7] used the term “information divergence” which expresses the non-uniform distribution of the visual information in an image for saliency detection. Several methods estimated saliency in superpixel level instead of pixel-wise level to reduce the computational time. Jiang et al. [8] performed salient object segmentation with multiscale super pixel-based saliency and a closed boundary prior. Their approach iteratively updates both the saliency map and the shape prior under an energy minimization framework.

Perazzi et al. [9] decomposed an image into compact and perceptually homogeneous elements, and then considered the uniqueness and spatial distribution of these elements in the CIE Lab color to detect salient regions. Yan et al. [10] used a hierarchical model by computing contrast features at different scales of an image and fused them into a single saliency map using a graphical model. Zhu et al. [11] proposed a background measure that characterizes the spatial layout of image regions with a novel optimization framework. These models tend to give a higher saliency at around edges and texture areas that have high contrasts, where humans tend to focus on in an image. However, these models tend to catch only parts of an object. Also, they tend to give non-uniform weight to the same salient object when different features presented in the same salient object. Global-contrast-based models use color contrast with respect to the entire image to detect salient regions. These models can detect salient regions of an image uniformly with low computational complexity.

Achanta et al. [12] proposed a frequency-tuned approach to determine the center-surround contrast using the color and luminance in the frequency domain as features. Shen and Wu [13] divided an image into two parts—a low-rank matrix and sparse noise—where the former explains the background regions and the latter indicates the salient regions. Cheng et al. [14] proposed a Gaussian mixture model (GMM)-based abstract representation method that simultaneously evaluates the global contrast differences and spatial coherence to capture perceptually

homogeneous elements and improve the salient region detection accuracy. Li et al. [15] showed that the unique refocusing capability of light fields can robustly handle challenging saliency detection problems such as similar foreground and background in a single image.

Borji and Itti [16] used complementary local and global patch-based dictionary learning for rarity-based saliency in different color spaces RGB and LAB and then combined them into the final saliency map for saliency detection. Jiang et al. [17] proposed a multilevel image segmentation method based on the supervised learning approach that performed a regional saliency regress or using regional descriptors to build a saliency map to find salient regions. These models are usually highly accurate and have a simple detection structure. However, they tend to require a lot of computational time. Therefore, superpixel-wise saliency detection is used to overcome the high computational complexity.

3. RELATED WORK

3.1 Efficient Salient Region Detection with Soft Image Abstraction

In this paper, we propose a novel soft image abstraction approach that captures large scale perceptually homogeneous elements, thus enabling effective estimation of global saliency cues. Unlike previous techniques that rely on super-pixels for image abstraction, we use histogram quantization to collect appearance samples for a global Gaussian Mixture Model (GMM) based decomposition. Components sharing the same spatial support are further grouped to provide a more compact and meaningful presentation. This soft abstraction avoids the hard decision boundaries of super pixels, allowing abstraction components with very large spatial support. This methods result is as shown in figure 2.

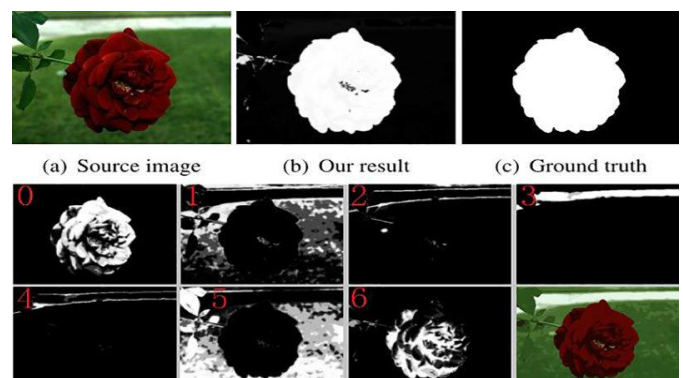


Fig -2: Soft image abstraction method to decompose an image into large scale.

This allows the subsequent global saliency cues to uniformly highlight entire salient object regions. Finally, we integrate the two global saliency cues, Global Uniqueness (GU) and Color Spatial Distribution (CSD), by

automatically identifying which one is more likely to provide the correct identification of the salient region. We extensively evaluate our salient object region detection method on the largest publicly available dataset with 1000 images containing pixel accurate salient region annotations [18]. The evaluation results show that each of our individual measures (GU and CSD) significantly outperforms existing 18 alternate approaches, and the final Global Cues (GC) saliency map reduces the mean absolute error by 25.2% compared to the previous best results, while requiring substantially less running times. In order to get an abstract global representation which effectively captures perceptually homogeneous elements, we cluster image colors and represent them using Gaussian Mixture Models (GMM). Each pixel color I_x is represented as a weighted combination of several GMM components, with its probability of belonging to a component c given by:

$$p(c | I_x) = \frac{\omega_c N(I_x | \mu_c, \Sigma_c)}{\sum_c \omega_c N(I_x | \mu_c, \Sigma_c)} \quad (1)$$

where ω_c , μ_c , and Σ_c represent respectively the weight, mean color, and covariance matrix of the c th component. We use the GMM to decompose an image in to perceptually homogenous elements. These elements are structurally representative and abstract away unnecessary details fig. 2 shows an example of such decomposition. Notice that our GMM-based representation better captures large scale perceptually homogeneous elements than superpixel representations which can only capture local homogeneous elements.

3.2 Frequency-tuned Salient Region Detection

The true usefulness of a saliency map is determined by the application. In this paper we consider the use of saliency maps in salient object segmentation. To segment a salient object, we need to binarize the saliency map such that one's (white pixels) correspond to salient object pixels while zeros (black pixels) correspond to the background. We present comparisons with our method against the five methods mentioned above. In the first experiment, we use a fixed threshold to binarize the saliency maps.

In the second experiment, [21] we perform image-adaptive binarization of saliency maps. In order to obtain an objective comparison of segmentation results, we use a ground truth image database. We derived the database from the publicly available database used by Liu et al. This database provides bounding boxes drawn around salient regions by nine users. However, a bounding box-based ground truth is far from accurate, as also stated by Wang and Li. Thus, we created an accurate object-contour based ground truth database of 1000 images. To analyze the properties of the five saliency algorithms, we examine the spatial frequency content from the original image that is retained in computing the final saliency map. It understands that the range of spatial frequencies retained by our proposed algorithm is more appropriate than the algorithms used for comparison. For simplicity, the

following analysis is given in one dimension and extensions to two dimensions are clarified when necessary.

In method IT, a Gaussian pyramid of 9 levels (level 0 is the original image) is built with successive Gaussian blurring and down sampling by 2 in each dimension. In the case of the luminance image, these results in a successive reduction of the spatial frequencies retained from the input image, its example is shown in figure 3. Each smoothing operation approximately halves the normalized frequency spectrum of the image. At the end of 8 such smoothing operations, the frequencies retained from the spectrum of the original image at level 8 range within $[0, \pi/256]$. The technique computes differences of Gaussian-smoothed images from this pyramid, resizing them to size of level 4, which results in using frequency content from the original image in the range $[\pi/256, \pi/16]$. In this frequency range the DC (mean) component is removed along with approximately 99% $((1 - \frac{1}{16^2}) \times 100)$ of the high frequencies for a 2-D image. As such, the net information retained from the original image contains very few details and represents a very blurry version of the original image.

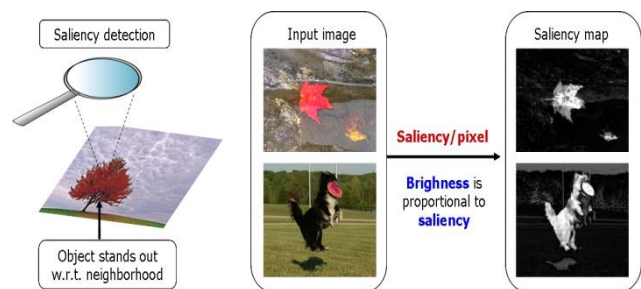


Fig -3: Frequency tuned salient region detection output.

3.3 Salient SLIC segmentation algorithm

Our approach [19] generates superpixels by clustering pixels based on their color similarity and proximity in the image plane. This is done in the five-dimensional $[labxy]$ space, where $[lab]$ is the pixel color vector in CIELAB color space, which is widely considered as perceptually uniform for small color distances, and xy is the pixel position. While the maximum possible distance between two colors in the CIELAB space (assuming RGB input images) is limited, the spatial distance in the xy plane depends on the image size. It is not possible to simply use the Euclidean distance in this 5D space without normalizing the spatial distances. In order to cluster pixels in this 5D space, we therefore introduce a new distance measure that considers superpixel size. Using it, we enforce color similarity as well as pixel proximity in this 5D space such that the expected cluster sizes and their spatial extent are approximately equal.

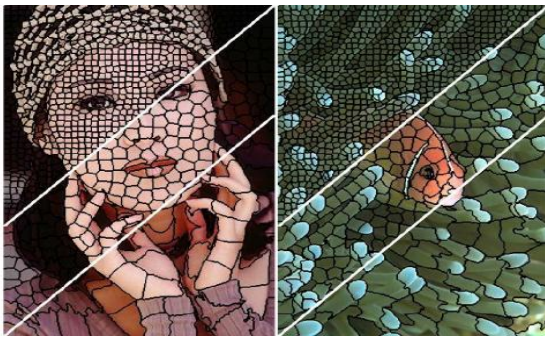


Fig -4: Using SLIC segmentation algorithm Superpixels generation.

Operating on superpixels instead of pixels can speed up existing pixel-based algorithms, and even improve results in some cases. For instance, certain graph-based algorithms can see a 2 to 3-fold speed increase using superpixels as shown in figure 4. Of course, the superpixel generation itself should be fast for this to be practical. Below, we consider two typical vision tasks that benefit from using superpixels: object class recognition and medical image segmentation. In each case, superpixels have been shown to increase the performance of an existing algorithm while reducing computational cost. We show that SLIC superpixels outperform state-of-the-art superpixel methods on these tasks, but with a lower computational cost.

3.4 High Dimension Color Transform Algorithm

In this section, we describe our method to detect the initial location of salient regions in an image. Our method [20] is a learning-based method and it processes an image in super pixel level. The initial saliency tri-map consists of foreground candidate, background candidate, and unknown regions. A similar approach has already been used in a previous method, which demonstrated superiority and efficiency in their results. However, their algorithms require considerable computational time because their features' computational complexity is very large. In our work, we only use some of the most effective features that can be calculated rapidly, such as color contrast and location features. As our goal in this step is to "approximately" find the salient regions of an image, we found that the salient region could be found accurately using even a smaller number of features. By allowing for the classification of some ambiguous regions as unknown, we can further improve the accuracy of our initial saliency trimap.

The location feature is used because humans tend to focus more on objects that are located around the centre of an image. Next, we concatenate histogram features as this is one of the most effective measurements for the saliency feature. The histogram features of the i th super pixel D_{Hi} is measured using the chi-square distance between other super pixels' histograms. It is defined as

$$D_{Hi} = \sum_{j=1}^N \sum_{k=1}^b \frac{(h_{ik}+h_{jk})^2}{(h_{ik}+h_{jk})'} \quad (2)$$

- Initial Saliency Trimap via Random Forest Classification

After we calculate the feature vectors for every superpixel, we use a classification algorithm to check whether each region is salient. In this study, we use the random forest classification because of its efficiency on large databases and its generalization ability. A random [3][6]forest is an ensemble method that operates by constructing multiple decision trees at training time and decides the class by examining each tree's leaf response value at test time.

$$D_{Li} = \sum_{j=1}^N \omega_{i,j}^p d(c_i, c_j) \quad (3)$$

$$\omega_{i,j}^p = \frac{1}{Z_i} \exp\left(-\frac{1}{2\sigma_p^2} \|P_i - P_j\|_2^2\right), \quad (4)$$

This method combines the bootstrap aggregating idea and random feature selection to minimize the generalization error. To train each tree, we sample the data with the replacement and train a decision tree with only a few features that are randomly selected. Typically, a few hundred to several thousand trees are used, as increasing the number of trees tends to decrease the variance of the model.

$$F_p = \frac{|(F_C) \cap (F_{GT})|}{|(F_C)|} \quad (5)$$

$$B_p = \frac{|(B_C) \cap (B_{GT})|}{|(B_C)|} \quad (6)$$

$$E_R = \frac{|((F_C) \cap (B_{GT})) \cup ((B_C) \cap (F_{GT}))|}{|I|} \quad (7)$$

4. RESULTS AND ANALYSIS

In this section of the thesis the precision plots, the recall plots and F-measure plots for different inputs of database like MSRA, PASCAL, and ECSSD have been calculated. Also to find working efficiency, sensitivity, specificity and eccentricity of this system plays important role for calculation. The precision plots obtained for this type of datasets explains the accuracy of detected saliency with respect to drawn ground truth. The recall plots obtained by comparing different database again and the analytical data show that, the data predicted from this comparison shows sensitivity of this method. The last section of this chapter is concluded with obtaining the normal comparative plots between old algorithm and ours experiment method. The details of the plots are explains in the one of the section.

4.1 PERFORMANCE ANALYSIS

In this section the performance analysis of HDCT method is described, results were obtained for the different database used for this method execution. The graphical plot of performance observation displays both the precision and recall analysis in the saliency of color images. Different images are used for experiments and graphical plots are shown. Plot command in MATLAB tool is use to create the 2-D graphical plots of the matrix data. The graphical plot explains the relation between the output saliency region accuracy and its sensitivity. Another plot describes about threshold and recall. Threshold of saliency map can be change manually this will effect on recall of final detected saliency map and thus we can conclude how sensitivity of detection changes as per threshold.

In HDCT code firstly input image is called from the path provided, HDCT method is applied over it its output is given in figure 5. By creating ground truth of given input manually and creating ground truth from HDCT method automatically, we are comparing both the ground truth on the basis of salient object area, salient object perimeter and salient object eccentricity. Further we are calculating its false negative value, true negative, false positive, true positive parameters, with accuracy, sensitivity and specificity. Different data sets of images like MSRA, PASCAL, and ECSSD these are specially used for image processing. Out of all images some selected images from every dataset were selected and applying this transforms to find out precision, recall and F-measure of every images. Plot of precision versus recall for every image in each dataset explains about precision of salient region extraction. And hence recall which is also termed as sensitivity is found out to be 0 to 0.4.

4.1.1 Performance Evaluation

In this calculation process, for evaluation of salient region detection algorithm precision-recall rate and F- measure rate were used. These evaluation criteria were proposed by Achanta *et al.* [12] and most saliency detection methods are evaluated by these criteria [16].

- 1) Precision-Recall Evaluation: The precision is also called the positive predictive value, and it is defined as the ratio of the number of ground truth pixels retrieved as the salient region to the total number of pixels retrieved as the salient region. The recall rate is also called the sensitivity and it is defined as the ratio of the number of ground truth regions. Two different approaches have been used to examine the precision-recall rate. The first approach is used to measure the rate for each pixel threshold. Bi-segment the saliency map

using every threshold from 0-255 and calculate precision rate.

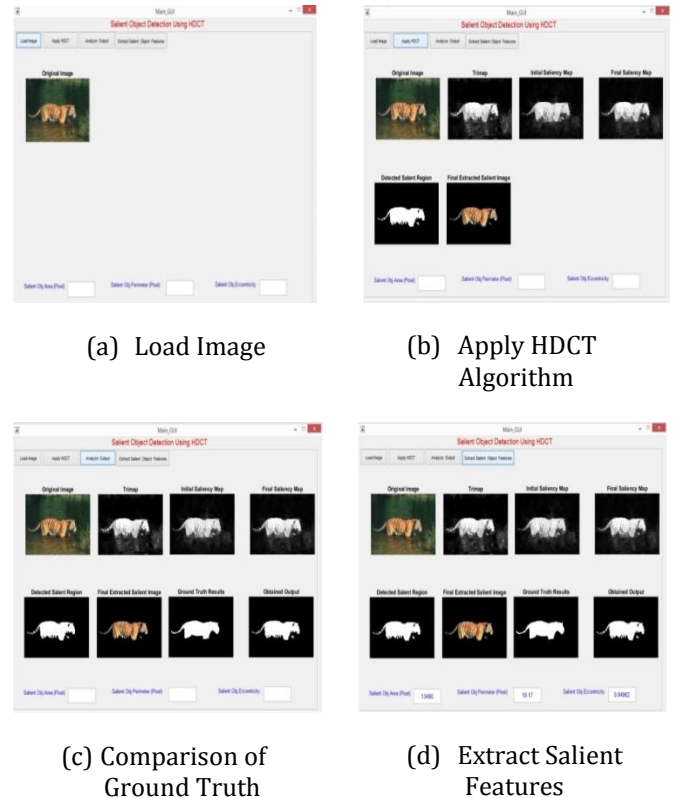


Fig -5 Figure Showing Stepwise Extracted Salient Features Using HDCT Method

4.2 STATISTICAL ANALYSIS

The evaluation of HDCT algorithm is based on three popular saliency databases: MSRA-B database, PASCAL-S and ECSSD database. The MSRA-B is a B image subset of MSRA database. These B images are excluding from database when learning the color prior, and which have been trained for different experimentation. Our approach is referring by using SLIC method for superpixel extraction as 'SS'.

For the first evaluation, a fixed threshold within [0, 255] is used to construct binary foreground mask from the saliency map. Then the binary mask is compared with the ground truth mask to obtain precision recall (P-R) pair. We work with different images from different database to find their precision and recall. This precision recall pair of different images for one algorithm helps to find efficiency, flexibility and F-measure of algorithm. Table 1, 2, 3 indicates P-R observations for all three databases respectively.

Table -1 Precision-Recall Observation of ECSSD Dataset by Using HDCT Method

| Input Image No. | Precision | Recall | F-measure |
|-----------------|-----------|--------|-----------|
| 1 | 0.99 | 0.09 | 0.16 |
| 2 | 0.98 | 0.10 | 0.18 |
| 3 | 1.00 | 0.37 | 0.54 |
| 4 | 0.75 | 0.09 | 0.16 |
| 5 | 0.97 | 0.10 | 0.18 |
| 6 | 1.00 | 0.30 | 0.46 |
| 7 | 0.82 | 0.11 | 0.18 |
| 8 | 0.49 | 0.16 | 0.24 |
| 9 | 0.54 | 0.11 | 0.19 |
| 10 | 1.00 | 0.16 | 0.27 |

Table -2 Precision-Recall Observation of MSRA Dataset by Using HDCT Method

| Input Image No. | Precision | Recall | F-measure |
|-----------------|-----------|--------|-----------|
| 1 | 0.66 | 0.33 | 0.44 |
| 2 | 1.00 | 0.26 | 0.41 |
| 3 | 0.55 | 0.29 | 0.38 |
| 4 | 1.00 | 0.38 | 0.55 |
| 5 | 0.72 | 0.11 | 0.19 |
| 6 | 0.34 | 0.15 | 0.21 |
| 7 | 0.99 | 0.17 | 0.29 |
| 8 | 0.95 | 0.31 | 0.47 |
| 9 | 0.12 | 0.12 | 0.11 |
| 10 | 0.29 | 0.15 | 0.20 |

Table -3 Precision-Recall Observation of PASCAL Dataset by Using HDCT Method

| Input Image No. | Precision | Recall | F-measure |
|-----------------|-----------|--------|-----------|
| 1 | 0.67 | 0.31 | 0.42 |
| 2 | 1.00 | 0.22 | 0.44 |
| 3 | 0.55 | 0.21 | 0.36 |
| 4 | 1.00 | 0.34 | 0.64 |
| 5 | 0.72 | 0.11 | 0.21 |
| 6 | 0.34 | 0.19 | 0.18 |
| 7 | 0.99 | 0.18 | 0.29 |
| 8 | 0.95 | 0.24 | 0.46 |
| 9 | 0.12 | 0.10 | 0.11 |
| 10 | 0.28 | 0.12 | 0.20 |

From P-R observation and from line graph figure 6 understands that precision for some images is observed to be nearly one this indicates salient region is extracted accurately.

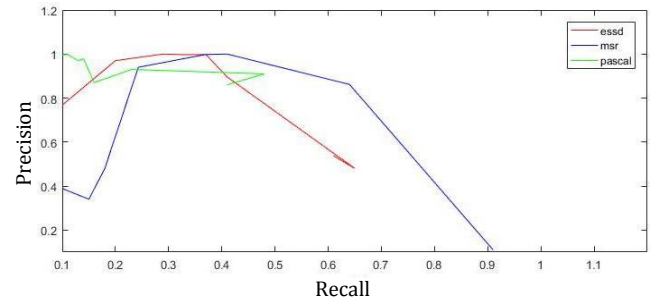


Fig -6 Graph Plot of Recall vs Precision of ECSSD, MSRA and PASCAL Image Datasets

Recall of some images lies between 0.1 and 0.4 this indicates that maximum precision minimum recall concept. Recall rate is not as important as precision for attention detection. For example, a 100% recall rate can be achieved by selecting whole image. From bar graph figure and from its line graph understand that MSRA database images have maximum calculated F-measure. Our approach reduces overall error rate on F-measure compare to CGVS method. Here $\beta=1$ is consider, β can be change from 0 to 1.

$$F_{\beta} = \frac{(1 + \beta^2) Precision \times Recall}{\beta^2 \times Precision + Recall}$$

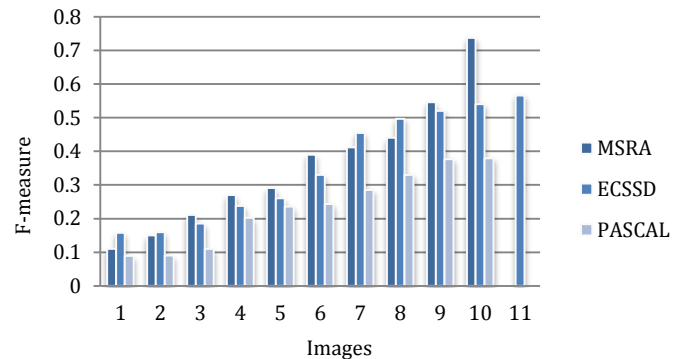


Fig -7 Bar Graph of Calculated F-measure of Different Images from MSRA, ECSSD and PASCAL Dataset

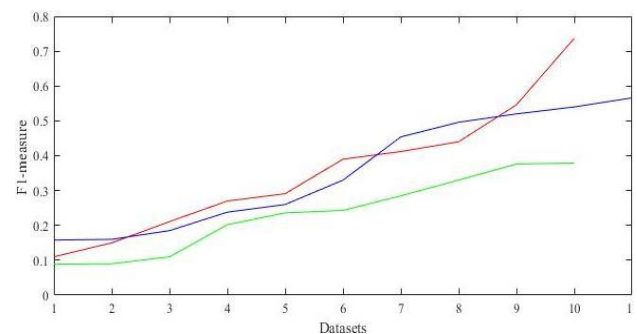


Fig -8 Graph of F₁- measure of Different Images from MSRA, ECSSD and PASCAL Dataset

Table -4 Measurement of True Negative, True Positive, False Negative and False Positive of Different Images

| Input Image | True Negative | True Positive | False Negative | False Positive | Accuracy |
|-----------------|---------------|---------------|----------------|----------------|----------|
| Bowl strawberry | 2.04 | 97.96 | 21.47 | 78.53 | 88.25 |
| Golden leaf | 16.72 | 83.28 | 47.47 | 52.53 | 67.90 |
| Cross in sand | 3.51 | 96.49 | 51.98 | 48.02 | 72.25 |
| Traffic board | 27.17 | 72.83 | 4.11 | 95.90 | 84.36 |

Table 4 describes about true positive, true negative, false positive and false negative of different images, which is obtained after comparison of generated ground truth and extracted salient region from method.

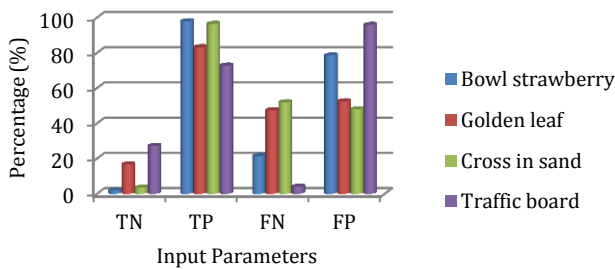


Fig -9 Graph Plot of True Negative, True Positive False Negative and False Positive in Percentage of Different Images

Table -5 Observation of Sensitivity, Specificity, Salient Object Area, Perimeter and Eccentricity of Images

| Input Image | Sensitivity | Specificity | Area (pixel) | perimeter | eccentricity |
|---------------|-------------|-------------|--------------|-----------|--------------|
| Bowl | 82.03 | 02.53 | 10209 | 807.84 | 0.96 |
| Golden leaf | 63.71 | 24.15 | 31276 | 1264.46 | 0.27 |
| Cross in sand | 64.99 | 06.81 | 5624 | 23.60 | 0.71 |
| Traffic board | 94.68 | 22.07 | 23168 | 1134.99 | 0.40 |
| Jumping boy | 87.93 | 03.83 | 17298 | 59.52 | 0.77 |
| Butterfly | 89.10 | 00.06 | 34914 | 1014.50 | 0.71 |
| Castle | 90.58 | 28.21 | 18698 | 79.69 | 0.81 |
| Lemon | 71.71 | 01.22 | 31691 | 1764.41 | 0.69 |
| Tiger | 92.94 | 07.11 | 13490 | 19.17 | 0.95 |

Table 5 describes about different parameters which are extracted during performance of this algorithm. It focuses on image sensitivity, specificity, perimeter, area occupied by salient region and calculation of eccentricity.

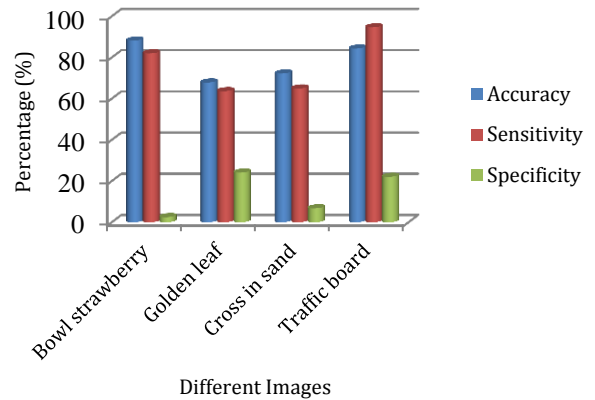


Fig -10 Graph Plot of Accuracy, Sensitivity and Specificity (in Percentage) of Extracted Salient Region by Applying HDCT Method to Different Images

4.3 COMPARATIVE ANALYSIS

In this section comparative analysis of proposed method is compared with the result of previous method. The results and statistical analysis of proposed method is discussed in previous section of this chapter. Figure 11 (a – e) is step wise output of previous method. Result of salient region detection using previous method depends on edge detection or edge pixels which are calculated by pixel positioning method. This method fails in detection of complete region and original colour extraction of typical area in image. But these drawbacks were solved by proposed method by using k-nearest pixel methodology and its result is shown in figure 11 (f – g).

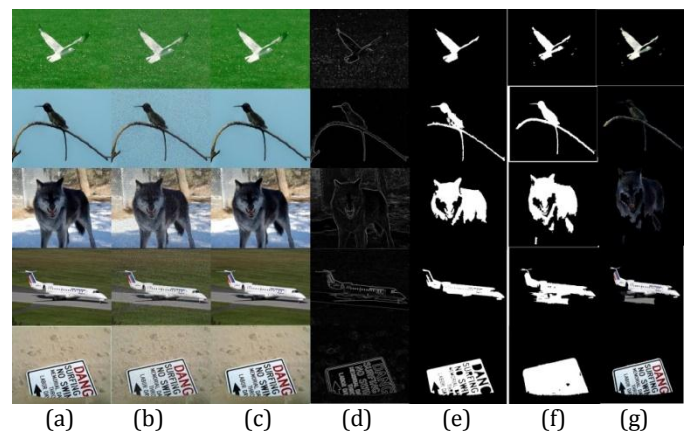


Fig -11 Different Image Saliency Extract Output by Contour Guided Visual Search Method (a-e) and High Dimension Colour Transform Method (f-g).

4.4 EXPERIMENTATION

The work on this project based on experimentation with three popular saliency databases: MSRA-B database, PASCAL-S and ECSSD database. The MSRA-B is a B image subset of MSRA database. These B images are exclude from database when learning the colour prior, and which have been trained for different experimentation. Our approach is referring by using SLIC method for superpixel extraction as 'SS'.

For the first evaluation, a fixed threshold within [0, 255] is used to construct binary foreground mask from the saliency map. Then the binary mask is compared with the ground truth mask to obtain precision recall (P-R) pair. We work with different images from different database to find their precision and recall. This precision recall pair of different images for one algorithm helps to find efficiency, flexibility and F-measure of algorithm. Table (1, 2, and 3) indicates P-R observations for all three databases respectively.

In first experimentation only one image is given to our algorithm. This is done by changing input parameter of image as shown in table 6. Parameters like Shadow that adjust dark color, Midtone that adjust midtones of image, Brightness adjust luminance of visual transmission in image or intensity of image, Contrast is the term refers to amount of colour or grayscale differentiation, Highlight; adjust light colours only.

From Experimentation I and II understands that our method detects most salient objects accurately it still has some limitations. For example, our HDCT might not fully coincide with human vision. However, it is still effective in increasing the success of foreground and background color separation as the low-dimensional RGB space is very dense where distribution of the foreground and background overlaps, whereas in high dimensional color space, the space is less dense and thus the overlap decreases as shown in table 6 and 7.























These matrices are then used to calculate sensitivity, specificity and accuracy as follows:

Sensitivity and specificity are statistical measures of the performance of a binary classification test, also known in statistics as classification function. Sensitivity also called the true positive rate, the recall, or probability of detection in some fields. It measures the proportion of positives that are correctly identified as such (i.e. the percentage of superpixels that are identified and extract correctly). Sensitivity refers to the method's ability that correctly detects saliency area with respect to original image. In the example of salient detection in image, the sensitivity of the method is the proportion of superpixels extracted with

help of trimap and results in positive detection. Mathematically, this can be expressed as:

$$sensitivity = \frac{\text{number of true positives}}{\text{number of true positives} + \text{number of false negatives}} \times 100$$

Table -6 Experimentation-I Represents Output Observation with Applying HDCT Algorithm on Single Image by Changing its Input Features like Shadow, Midtone, Brightness, Contrast and Highlight

| Input | Shadow | Midtone s | Brightness | Contrast | Highlight | Output |
|---|--------|-----------|------------|----------|-----------|---|
|  | 0 | 0 | 0 | -30 | 0 |  |
|  | -100 | 40 | 30 | -30 | -90 |  |
|  | 0 | 0 | -30 | 0 | 0 |  |
|  | 0 | 0 | 0 | -80 | 0 |  |
|  | 0 | 0 | 0 | 100 | 0 |  |
|  | 0 | 0 | -60 | 0 | 0 |  |
|  | 0 | 0 | 30 | 0 | 0 |  |
|  | 0 | 0 | 50 | 0 | 0 |  |
|  | 0 | 0 | 0 | 0 | 100 |  |
|  | 0 | -100 | 0 | 0 | 0 |  |
|  | 100 | 0 | 0 | 0 | 0 |  |




$$sensitivity = \text{probability of a correctly detected salient area in image}$$

$$Sensitivity = \frac{TP}{TP + FN} \times 100$$

$$Specificity = \frac{TN}{TN + FP} \times 100$$

$$Accuracy = \frac{(TP + FP)}{2}$$

Table -7 Experimentation-II Output Observation Carried Out With HDCT Algorithm on Single Image by Changing its Hue, Saturation and Amount in Input

| Input image | Hue | Saturation | Amount | Output image |
|---|------|------------|-------------|---|
|  | 0 | 0 | 0 |  |
|  | 0 | 0 | 50 |  |
|  | 50 | 0 | 50 |  |
|  | 100 | 0 | 50 |  |
|  | 180 | 0 | 50 |  |
|  | -100 | 0 | 100 (white) |  |
|  | 0 | 100 | 0 |  |
|  | 0 | -100 | 0 |  |
|  | 0 | 100 | 100 |  |

Specificity tells us how likely the test images are unambiguous or how specific image is extracted compare to generated ground truth. Accuracy of image is calculated which state that the quality of image being true, correct or exact, more precise.

5. CONCLUSIONS

Object detection is necessity of picture handling process in image processing. In this paper we survey the current systems of salient object detection. Salient region detection is a challenging problem and an important topic in computer vision. The single visual cue based salient region detection methods have their own limitation. Implementation of HDCT method deals with salient region detection that estimates the foreground regions from a trimap using two different methods: global saliency estimation via HDCT and local saliency estimation via regression. The trimap-based robust estimation overcomes the limitations of inaccurate initial saliency classification. As a result, this method achieves good

performance and is computationally efficient in comparison to the state-of-the art methods.

The experimental results show that our algorithm is effective and computational efficient. Although computational speed is slower than previous methods but it indicates that as initial trimap when generated accurately then this method has potential to obtain better result. Calculation of Precision and recall for different database is depend on threshold value which is set while performance. Threshold value is defined as two times the mean value of the saliency map. It is found that some test images of PASCAL database has salient object larger than background then two times the mean value of saliency map is not suitable for thresholding, it needs adaptive thresholding.

After experimentation on HDCT algorithm it is found that the most salient object in an image is produce efficiently. This overcomes the drawback of sub-optimal results for images with multiple objects, and can be useful for those applications requiring high detection rate with cluttered scenes. Foreground and background colour separation as the low dimensional RGB space is very dense where distributions of the foreground and background colors overlap, whereas in high-dimensional color space, the space is found to be less dense and overlap decreases.

REFERENCES

- [1] Z. Liu, R. Shi, L. Shen, Y. Xue, K. N. Ngan, and Z. Zhang, "Unsupervised salient object segmentation based on kernel density estimation and two-phase graph cut," IEEE Trans. Multimedia, vol. 14, no. 4, pp. 1275–1289, Aug. 2012.
- [2] V. Navalpakkam and L. Itti, "An integrated model of top-down and bottom-up attention for optimizing detection speed," in Proc. IEEE Conf. Comput. Vis. Pattern Recognit. (CVPR), Jun. 2006, pp. 2049–2056.
- [3] L. Itti, J. Braun, D. K. Lee, and C. Koch, "Attentional modulation of human pattern discrimination psychophysics reproduced by a quantitative model," in Proc. Conf. Adv. Neural Inf. Process. Syst. (NIPS), 1998, pp. 789–795.
- [4] J. Harel, C. Koch, and P. Perona, "Graph-based visual saliency," in Proc. Conf. Adv. Neural Inf. Process. Syst. (NIPS), 2006, pp. 545–552.
- [5] S. Goferman, L. Zelnik-Manor, and A. Tal, "Context-aware saliency detection," in Proc. IEEE Conf. Comput. Vis. Pattern Recognit. (CVPR), Jun. 2010, pp. 2376–2383.
- [6] A. Klein and S. Frntrop, "Center-surround divergence of feature statistics for salient object detection," in Proc. IEEE Int. Conf. Comput. Vis. (ICCV), Nov. 2011, pp. 2214–2219.

- [7] W. Hou, X. Gao, D. Tao, and X. Li, "Visual saliency detection using information divergence," *Pattern Recognit.*, vol. 46, no. 10, pp. 2658–2669, Oct. 2013
- [8] H. Jiang, J. Wang, Z. Yuan, T. Liu, and N. Zheng, "Automatic salient object segmentation based on context and shape prior," in *Proc. Brit. Mach. Vis. Conf. (BMVC)*, 2011, pp. 110.1–110.12.
- [9] F. Perazzi, P. Krahenbuhl, Y. Pritch, and A. Hornung, "Saliency filters: Contrast based filtering for salient region detection," in *Proc. IEEE Conf. Comput. Vis. Pattern Recognit. (CVPR)*, Jun. 2012, pp. 733–740.
- [10] Q. Yan, L. Xu, J. Shi, and J. Jia, "Hierarchical saliency detection," in *Proc. IEEE Conf. Comput. Vis. Pattern Recognit. (CVPR)*, Jun. 2013, pp. 1155–1162.
- [11] W. Zhu, S. Liang, Y. Wei, and J. Sun, "Saliency optimization from robust background detection," in *Proc. IEEE Conf. Comput. Vis. Pattern Recognit. (CVPR)*, Jun. 2014, pp. 2814–2821.
- [12] R. Achanta, S. Hemami, F. Estrada, and S. Susstrunk, "Frequency-tuned salient region detection," in *Proc. IEEE Conf. Comput. Vis. Pattern Recognit. (CVPR)*, Jun. 2009, pp. 1597–1604. *IEEE transactions on image processing*, vol. 25, January 2016.
- [13] X. Shen and Y. Wu, "A unified approach to salient object detection via low rank matrix recovery," in *Proc. IEEE Conf. Comput. Vis. Pattern Recognit. (CVPR)*, Jun. 2012, pp. 853–860.
- [14] M.-M. Cheng, J. Warrell, W.-Y. Lin, S. Zheng, V. Vineet, and N. Crook, "Efficient salient region detection with soft image abstraction," in *Proc. IEEE Int. Conf. Comput. Vis. (ICCV)*, Dec. 2013, pp. 1529–1536.
- [15] N. Li, J. Ye, Y. Ji, H. Ling, and J. Yu, "Saliency detection on light field," in *Proc. IEEE Conf. Comput. Vis. Pattern Recognit. (CVPR)*, Jun. 2014, pp. 2806–2813
- [16] A. Borji and L. Itti, "Exploiting local and global patch rarities for saliency detection," in *Proc. IEEE Conf. Comput. Vis. Pattern Recognit. (CVPR)*, Jun. 2012, pp. 478–485.
- [17] H. Jiang, J. Wang, Z. Yuan, Y. Wu, N. Zheng, and S. Li, "Salient object detection: A discriminative regional feature integration approach," in *Proc. IEEE Conf. Comput. Vis. Pattern Recognit. (CVPR)*, Jun. 2013, pp. 2083–2090.
- [18] R. Achanta, A. Shaji, K. Smith, A. Lucchi, P. Fua, and S. Süssstrunk, "SLIC superpixels compared to state-of-the-art superpixel methods," *IEEE Trans. Pattern Anal. Mach. Intell.*, vol. 34, no. 11, pp. 2274–2282, Nov. 2012.
- [19] J. Kim, D. Han, Y.-W. Tai, and J. Kim, "Salient region detection via high-dimensional color transform," in *Proc. IEEE Conf. Comput. Vis. Pattern Recognit. (CVPR)*, Jun. 2014, pp. 883–890.